PHYSICAL REVIEW B VOLUME 9, NUMBER 11 1 JUNE 1974

Auger satellites of the $L_{2,3}$ Auger emission bands of Al, Si, and P†

J. J. Melles*, L. E. Davis‡, and L. L. Levenson
Department of Physics and Graduate Center for Materials Research, University of Missouri-Rolla, Rolla, Missouri 65401
(Received 1 October 1973)

In this study a detailed investigation of the high-energy satellites of the $L_{2,3}$ Auger emission bands of Al, Si, and P was made. The satellites are interpreted as arising from double ionization of the $L_{2,3}$ shell rather than from a plasmon gain process. The parent-to-satellite energy separations ΔE between like structures were determined and were found to be consistently smaller than the volume-plasmon energies measured for the same samples. A comparison of Si and SiO revealed no evidence that ΔE for Si is dependent on the volume-plasmon energy of the sample. The satellite threshold excitation energies E_t were determined and were found to compare well with results expected for double ionization of the $L_{2,3}$ level. In the energy range $E_t < E_p \leq 2$ KeV the ratio of the satellite-to-parent Auger intensities for all three samples was in good agreement when plotted vs the reduced energy scale, E_p/E_t. The results were also found to be consistent with Gryzinski's binary-encounter model. If satellites in the Auger spectrum arise from double ionization of an inner-core level, then a corresponding ionization-loss peak should be present in the characteristic loss spectrum associated with the elastic peak. An ionization-loss peak was found for Si at a loss energy of 216 eV and is tentatively identified as a loss peak associated with double ionization of the $L_{2,3}$ shell.

I. INTRODUCTION

Recent studies of the $L_{2,3}$ Auger emission bands of Mg,[1] Al,[2,3] and Si[4,5] have shown the presence of high-energy satellite peaks. In addition we have also observed a similar satellite for P.[6] These weak structures appear to be identical to x-ray satellites which have been previously reported on the high-energy side of the $L_{2,3}$ emission bands of Na, Mg, Al, and Si.[7] It has been suggested that these peaks in Auger and x-ray spectra might arise from the double ionization of the $L_{2,3}$ shell resulting in a shift of the emission band to higher energies in both cases.[8,9] Hanson and Arakawa[7] have shown in a study of x-ray satellites that the observed shift is in agreement with that expected assuming double ionization.

An alternate explanation proposed is that the shift is a result of a volume-plasmon gain process.[5,10] Recently Watts[11] has suggested that the dynamical screening of a core hole by the conduction electrons can yield a plasmon gain peak in the Auger spectra of a metal. A calculation made for Al, assuming a core lifetime of 8×10^{-16} sec, predicted a plasmon gain peak comparable in magnitude to that observed. As noted by Chung and Jenkins[1,2,5] and other workers, the general agreement between the observed volume-plasmon energies and the observed shifts also gives credence to the possibility of a plasmon gain process. However, Rowe and Christman[12] have recently reported Auger results for Si that strongly indicate that a plasmon mechanism is not responsible. They found that the Auger spectra of Si and SiO exhibited identical spacings of 15 eV between the parent and satellite bands although the volume-plasmon energies are 17 and 22 eV, respectively. Also, the primary excitation threshold for the satellite was determined and found to be in good agreement with that expected for double ionization.

The identification of these satellites then is of interest from the point of view of identifying possible inner-shell ionization and deexcitation mechanisms. The possibility that collective effects in the form of coupling between valence electrons and the core hole might be involved in deexcitation is of particular interest.

In the present work electron-induced Auger electron spectroscopy (AES) was used to study the higher-energy satellites of the $L_{2,3}VV$ Auger transition for Al, Si, and P. Since the initiation of an Auger transition depends upon the ejection of an inner-shell electron (in this case the $L_{2,3}$ shell), Auger spectra as well as the ionization-loss spectra can be used to study inner-shell-ionization cross sections. By determining the incident threshold energy necessary to produce the transition one can determine the core level involved. Hence, investigating Auger intensities as a function of incident excitation energy should clearly distinguish between double ionization of the $L_{2,3}$ shell and a process involving dynamical screening of a single $L_{2,3}$ shell vacancy.

In addition, since ionization-loss peaks associated with the elastic peak are observed for the $L_{2,3}$ and L_1 shells, it might also be possible to observe such a peak resulting from double ionization of the $L_{2,3}$ level.

The results of this investigation are shown to give strong support to the explanation in terms of double ionization. In Sec. III A of this paper we compare the observed shifts of the satellite band with the volume-plasmon energies for Al, Si, SiO, and P. In Sec. III B, the results of measuring the

threshold primary excitation energy necessary for producing the high-energy satellites will be reported and compared to that expected for double ionization of the $L_{2,3}$ shell. In Sec. III C, the ratio of the satellite-to-parent intensities as a function of the incident-electron energy will be compared with the ratio of double-to-single ionization cross sections based on the classical theory of Gryzinski.[13] Finally, in Sec. III D, the characteristic energy-loss spectrum associated with the elastic peak is examined for Si and evidence of an ionization-loss peak corresponding to the double ionization energy of the $L_{2,3}$ level is reported.

II. EXPERIMENTAL DETAILS

The experimental arrangement used has been discussed in previous reports but is reproduced here for convenience.[14] The chamber was a stainless-steel bell jar which could be evacuated to pressures on the order of 3×10^{-10} Torr after a 24-h bake at 225 °C using a liquid-nitrogen-trapped oil diffusion pump. Total pressures were measured with a Bayard-Alpert ionization gauge and partial pressures with a monopole mass spectrometer. The main residual gases were found to be H_2 ($P_{H_2} \simeq \frac{1}{2} P_{CO}$), CO, and CO_2 ($P_{CO_2} \simeq \frac{1}{2} P_{CO}$). No mass above 44 amu was detected with a detectability of $P \leq 10^{-11}$ Torr.

To enable rotation, translation, and tilt motions to be made, a multiple sample carrier was mounted on a vacuum manipulator such that the samples could be positioned in front of the Auger electron spectrometer or the evaporation sources. The multiple sample carrier (previously described)[14] provided both shielding of the AES optics from the evaporation sources and an electron bombardment oven capable of up to 100 W power for thermal cleaning of samples.

An Auger electron spectrometer of the type described by Palmberg, Bohn, and Tracy[15] was used. It consisted of a cylindrical mirror analyzer (CMA) with a coaxial electron gun and a CuBe electron multiplier. The analyzer had a constant energy resolution of approximately 1%.

Positioning of the sample at the focus of the analyzer was accomplished by adjusting for a symmetric elastic peak of maximum peak height. The applied voltage to the mirror electrode of the CMA was monitored with a digital voltmeter. The proportionality factor between the analyzer pass energy and the applied voltage was determined by using the elastic peak for calibration.[16] This allowed the relative energy scale to be determined to within 1% for the parent-satellite separation energies and the plasmon-loss energies reported in Sec. III A.

The Auger electron spectra were taken in either the $dN(E)/dE$ or the $d^2N(E)/dE^2$ modes by detecting the first or second harmonic of the modulation frequency. The detected frequency in either mode of operation was 30 kHz while the frequency of the applied modulation were 30 and 15 kHz, respectively. The usual electronic signal processing equipment for synchronous detection was used.[15]

The satellite to parent Auger intensity ratios were measured as a function of the incident-beam energy for the three materials studied in order to obtain threshold energies for the satellite peaks in Sec. III B as well as the relative yield versus excitation energy in Sec. III C. In order to reduce the secondary-electron background for primary energies near threshold, the second derivative of the energy distribution was recorded. The satellite-to-parent Auger intensity ratio was then taken as being proportional to the ratio of the peak-to-peak heights between the minimum and the second maximum in the second derivative. The pass energy was modulated by 7.5 eV peak to peak.

By using ratios, beam-energy-dependent corrections such as the secondary-electron enhancement factor and the range of the primary electrons were reduced to negligible proportions. In addition, the use of ratios effectively normalized out the beam current and geometrical factors. This allowed the data to be taken in a more reproducible way and also eliminated the problem of a beam diameter which varied with beam current at the lower voltages. The latter problem showed up in current normalization. We were unable to obtain a constant Auger signal per unit incident beam current as a function of beam current at a fixed low beam voltage.

For silicon, a high resistivity (> 1000 Ω cm) silicon (111) wafer was used. Initial cleaning was accomplished by heating at 1200 °C for 5 min after which the only remaining impurity observed by AES was carbon (estimated at 0.1 monolayer). Subsequent cleaning was possible at lower temperatures and shorter time intervals. In a previous study using low-energy-electron diffraction, this same cleaning technique produced the well-recognized Si(111) 7×7 pattern.[17]

The phosphorus sample was produced by evaporating a thick phosphorus film onto a silicon substrate using a GaP (99.999% pure) evaporation source previously described.[17] After outgassing, a pressure of $\leq 2\times10^{-9}$ Torr could be maintained during evaporation. Impurities detectable on a freshly evaporated surface include gallium (20%), carbon (6%), and oxygen (< 0.8%).

An aluminum sample was made by evaporation of 99.99%-pure aluminum from an outgassed 0.007-in. W filament onto a thermally cleaned Ta substrate. During evaporation a pressure $\leq 5\times10^{-9}$ torr was maintained. Initially, aluminum was evaporated until the oxygen peak was no longer detectable (< 1%). Some carbon and sulfur were found at concentrations of 8% and 1%, respectively.

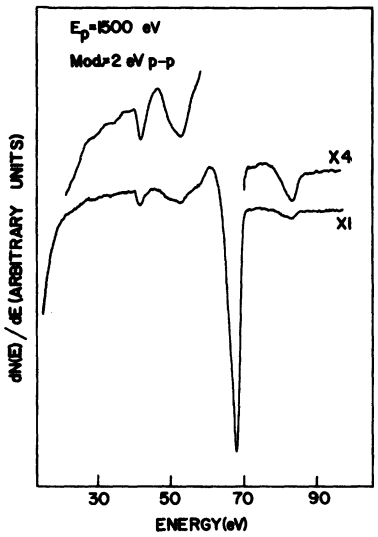

FIG. 1. $L_{2,3}$ Auger-emission band of Al.

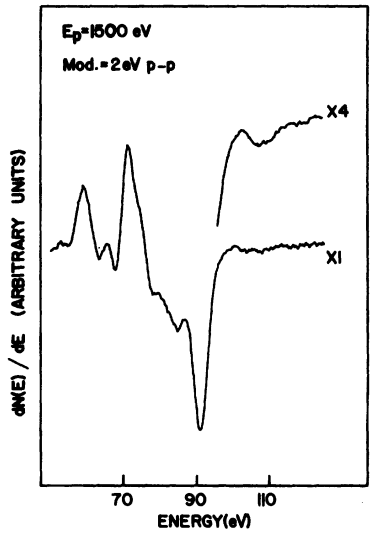

FIG. 3. $L_{2,3}$ Auger-emission band of SiO.

The above impurity estimates were made in the manner of Ueda and Shimizu[18] to within a factor of 2 using a beam voltage of 1500 V and a beam current of 30 μA. The Auger intensities were corrected for relative analyzer window width, relative sensitivity (using Gryzinski's cross section formula),[13] and estimated escape depth.[19]

Each freshly evaporated phosphorus or aluminum surface was used for about 4 h. In this time period no change in shape of the $L_{2,3}$ VV Auger spectrum of either sample was observed. The only degradation observable was approximately a 10% decrease in signal amplitude.

III. RESULTS AND DISCUSSION

A. Parent-to-satellite energy separations

The region of the $L_{2,3}$ Auger emission band and associated high-energy satellite peak for Al, Si, SiO, and P are shown in Figs. 1–4. The satellite structures are located at 83 eV for Al, 106 eV for Si, and 136 eV for P. The comparisons presented in this study were made between the principle peak in the parent band located at the top of the band and the satellite structure. The two bands are assumed to overlap with the satellite structure being just a

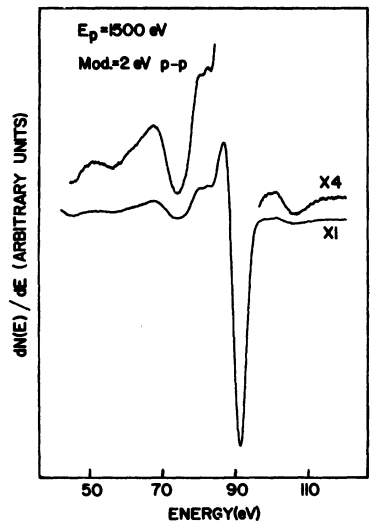

FIG. 2. $L_{2,3}$ Auger-emission band of Si(111).

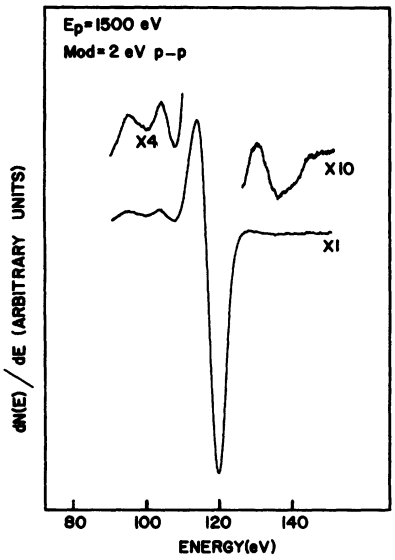

FIG. 4. $L_{2,3}$ Auger-emission band of P.

reflection of the principle peak and hence representing the top of the shifted satellite band. The spectra presented agree well with those previously cited.

Because of the considerable amount of gallium observed in the phosphorus spectrum there might be some question as to the identification of the small peak at 136 eV as being due to phosphorus or gallium. Uebbing and Taylor did observe a weak transition for GaAs at 129 eV which they assigned as an M_1M_4V gallium transition.[20] However, using the M_2M_4V gallium transition at 78 eV for comparison it is estimated that the M_1M_4V transition is less than 5% of the observed structure. Hence the gallium contribution is negligible and the observed structure is apparently a satellite of phosphorus similar to those already reported for Mg, Al, and Si.

It was found that there is some difficulty in determining ΔE between like structures in the parent and satellite bands. The energy separations were measured in both the $dN(E)/dE$ and the $d^2N(E)/dE^2$ operating modes and the results are shown in Table I. The shift obtained from the $dN(E)/dE$ spectra is taken to be between the inflections on the high-energy side. The energy separation between minima in the $d^2N(E)/dE^2$ spectra represents the separation between the peak positions of the parent and satellite bands. It is found that the values of ΔE seen in the $d^2N(E)/dE^2$ operating mode are somewhat smaller than the x-ray results[7] and those obtained from $dN(E)/dE$ spectra. This broadening might be indicative of plasmon dispersion. However, double ionization would also give this result due to lifetime effects. In addition, double ionization of the $L_{2,3}$ core level would be expected to result in splitting the state to $^3P_{210}$, $^1D_2$, and $^1S_0$ states. Structures seen in x-ray satellites have seen attributed to this splitting,[7] although such structure has not been observed in Auger spectroscopy.

Also shown in Table I are the observed volume-plasmon energies from our measurements on the characteristic-loss spectra for each of the samples used. These are found to be in good agreement with those obtained by others. The parent-to-satellite energy separations ΔE are seen to be comparable in magnitude with the volume-plasmon energies. It is this general agreement which has given support to the plasmon-gain interpretation. However, an analysis based on energy considerations alone is not sufficient to establish the identity of the satellites. As pointed out in Sec. I, Hanson and Arakawa[7] in a paper on high-energy x-ray satellites for Na, Mg, Al, and Si have shown that the observed energy separation ΔE is also in good agreement with that expected from double ionization of the $L_{2,3}$ shell.

TABLE I. Energy separation between satellite and parent $L_{2,3}$ bands.

Material	ΔE $\frac{dN(E)}{dE}$ data (eV)	ΔE $\frac{d^2N(E)}{dE^2}$ data (eV)	ΔE X-ray results[a] (eV)	Volume-plasmon energy (eV)
Al	15.7 ± 0.5	14.0 ± 0.5	15.2 ± 0.3	15.7
Si	15.6 ± 0.5	14.7 ± 0.5	16.1 ± 0.3	17.2
SiO		15 ± 1		20.1
P	16.2 ± 0.5	15.5 ± 0.5		18.4

[a]From Ref. 7.

A comparison between Si and oxidized Si, moreover, reveals no relation between the observed energy separation and the volume-plasmon energies. This agrees with the findings of Rowe and Christman[12] for Si and SiC. Thus the satellite for Si appears not to be a property of the compound in which Si is found.

B. Satellite threshold energies

In this section we will examine the behavior of the satellites as a function of the primary excitation energy. The data were obtained using the second derivative of the electron energy distribution $N(E)$ in order to effectively reduce the secondary-electron background in the measurement of the small satellite peak.[21] The first- and second-derivative curves of the Si Auger spectra at a beam voltage of 250 V is shown in Fig. 5. The background is considerably flatter in the second-derivative curve. The Auger current was taken as being proportional to the peak-to-peak height between the minimum and the second maximum in the second derivative for both the parent and satellite peaks.

We can also comment about some other features observed in the spectra of Fig. 5. Just to the high-energy side of the Si 92-eV peak is a small inflection which we believe marks the upper-band threshold.[22] It is not observable at higher beam energies and has not been previously reported. Presumably it is obscured at higher beam energies because of the overlapping of the satellite and parent bands.

The three structures observable at energies of 7, 11, and 18 eV below the $L_{2,3}$ ionization-loss peak have been previously reported by us.[6] This structure is possibly due to characteristic losses as is seen in the characteristic-loss spectrum of the elastic peak and/or due to electron shake off[23] of the valence-shell electrons occurring with the $L_{2,3}$ ionization process. Also present is a plasmon related loss which we will discuss more in Sec. III D.

In Fig. 6 we have plotted the normalized ratio of I_s/I_p vs primary excitation energy E_p for Al, Si, and P. Here I_s is the Auger-current yield for the satellite and I_p that of the parent peak. Representa-

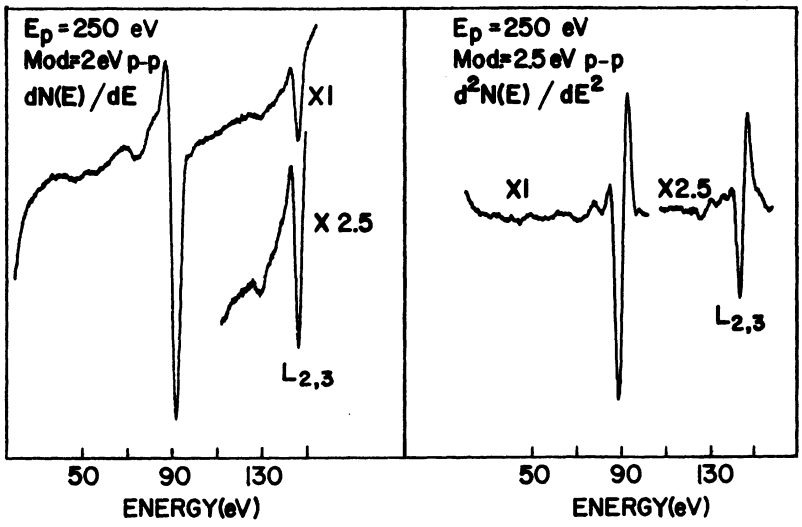

FIG. 5. Si(111) Auger spectrum obtained by using the $dN(E)/dE$ and the $d^2N(E)/dE^2$ operating modes.

tive error bars are shown for Si, the main errors being due to shot noise and a background correction which was still large near threshold even though double differentiation was performed.

The data for Si and P appear to be linear near threshold and a linear extrapolation was made to determine the threshold energy. These values are given in Table II. Background corrections were determined for Si and the same corrections were applied to P. In the case of Al, however, the data do not approach as close to threshold as it does for Si and P.

A lower sensitivity occurs at low beam voltages due to a reduced electron-gun current. An additional problem is that as the beam voltage is lowered to near threshold, the multiple plasmon losses seen below the elastic peak begin to interfere with the observation of the satellite peak.

Consequently, it was not possible to obtain a meaningful extrapolation for Al. Rather, the threshold was estimated as being given by $E_{peak}/5 = 800/5$ eV $= 160$ eV, where E_{peak} is the incident excitation energy at the position of the I_s/I_p peak. The factor of $\frac{1}{5}$ is that observed for Si and P.

The experimental thresholds are compared to those expected from a double-ionization theory in Table II. The energy needed for double ionization of the $L_{2,3}$ shell is denoted by $E_{(L_{2,3})^2}$. The first estimate shown, $E^1_{(L_{2,3})^2}$, was obtained by analogy with the Burhop formula for Auger transitions. This estimate is simply given by

$$E^1_{(L_{2,3})^2}(Z) = E_{L_{2,3}}(Z) + E_{L_{2,3}}(Z+1) \ , \qquad (1)$$

where $E_{L_{2,3}}(Z)$ is the binding energy of the $L_{2,3}$-shell electrons for element of atomic number Z. This estimate should be an upper limit. The experimental data itself yield a second estimate. Here we take

$$E^2_{(L_{2,3})^2}(Z) = 2E_{L_{2,3}}(Z) + \Delta E(Z) \ , \qquad (2)$$

where $\Delta E(Z)$ is the observed displacement of the satellite band. The $L_{2,3}$ binding energies were taken from Bearden and Burr.[24] The general agreement is observed to be good.

It is also evident that the threshold potential obtained for the phosphorus satellite (271 eV) is considerably higher than the gallium M_1 core-level energy (181 eV)[24] which gives rise to the weak M_1M_4V transition reported in the energy region of the observed satellite. This supports our earlier contention that the M_1M_4V gallium Auger transition was weak and that the structure observed was indeed a satellite of the $L_{2,3}$ Auger emission band of phosphorus.

C. Ratio of satellite-to-parent intensities

Ionization cross sections for single and double ionization of the $L_{2,3}$ shell by electron impact can be calculated using Gryzinski's binary-encounter theory.[13] Gryzinski's mathematical formulation has been criticized for some unrealistic features.[25] Our approach here is to consider this model as a semiempirical formulation as has been previously suggested.[25] The formulas obtained by Gryzinski

TABLE II. Primary excitation threshold energies for the $L_{2,3}$ emission-band satellites.

Material	E_t (eV)	$E_t/E_{L_{2,3}}$	$E^1_{(L_{2,3})^2}$ (eV)	$E^2_{(L_{2,3})^2}$ (eV)
P	271 ± 15	2.1	297	279
Si	212 ± 15	2.1	231	212
Al	160 (est.)	2.2	172	159

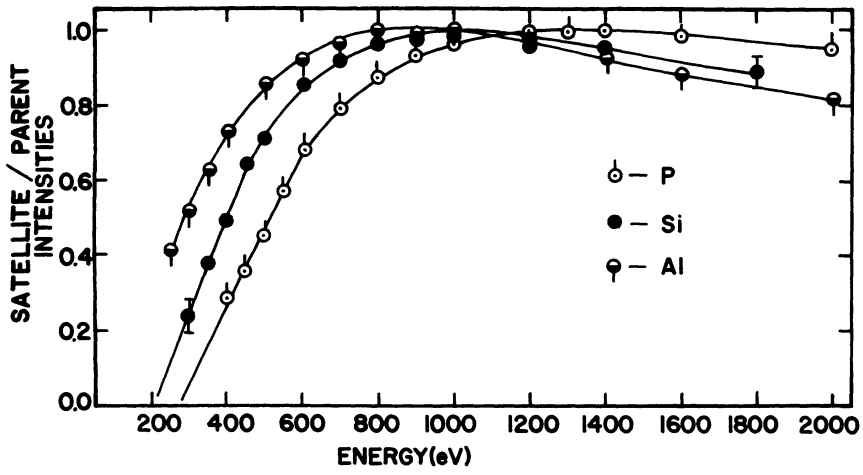

FIG. 6. Plot of the normalized satellite to parent Auger intensity ratios vs the primary beam energy for Al, Si, and P. (Smooth curves have been drawn for clarity.)

appear to have been sufficiently tested to be reliable for the comparison we wish to make. It has been demonstrated recently by several workers that the formula derived from this model for single ionization is in good agreement with experimental K- and $L_{2,3}$-shell ionization cross sections for light elements.[22,26] In addition, calculations of double-ionization cross sections for the valence shell using Gryzinski's relation has produced reasonably good agreement with experimental data for the rare gases and alkali-metal ions.[27,28]

The expression derived for the double-ionization cross section is[13]

$$Q_{II}=\frac{nN(N-1)(\pi e^4)^2}{4\pi\bar{d}^2 U_i^2 U_{ii}^2}[g_{sc}^{ii}+g_{ej}^{ii}] \ , \tag{3}$$

where n is the number of atoms per unit volume, N is the number of electrons in the shell in which the initial ionization occurs, e is the electronic charge, $\bar{d}$ is the mean distance between electrons in the shell, U_i and U_{ii} are the first- and second-ionization potentials, and E_p is the incident electron energy. In the binary-encounter theory double-electron ejection involves a double binary encounter. The function g_{sc}^{ii} represents that component of the cross section arising from two successive collisions of the incident electron while g_{ej}^{ii} is that due to a collision between the first ejected electron and those remaining. It is these two terms which contain the dependence of the cross section on E_p. They are defined by the relations

$$g_{sc}^{ii}=\left[g(B;x)-\left(\frac{1}{x-f}\right)^2 g\left(\frac{B}{x-f};\frac{x}{x-f}\right)\right] g\left(\frac{B}{f};\frac{x}{f}-\frac{(x-f)\ln(x-f)}{f(x-f-1)}\right) \ ,$$

$$g_{ej}^{ii}=\left(\frac{1}{1+f}\right)^2 g\left(\frac{B}{1+f};\frac{x}{1+f}\right) g\left(\frac{B}{f};\frac{(1+f)x\ln[x/(1+f)]}{(x-1-f)f}-\frac{1}{f}\right) \ , \tag{4}$$

where

$$x=E_p/U_i \ ,$$

$$B=E_1/U_i \ ,$$

$$f=U_{ii}/U_i \ ,$$

and

$$g(u;v)=\frac{u}{v}\left(\frac{v}{v+u}\right)^{3/2}\left(\frac{v-1}{v}\right)^{(2u+1)/(u+1)}\left(\frac{1}{u}+\tfrac{2}{3}(1-1/2v)\ln[2.7+(v-1)/u]^{1/2}\right) \ .$$

In the above expression for B, E_1 is the expectation value of the kinetic energy of the bound electron.

Using the same notation, the cross section for single ionization is given by[13]

$$Q_I=\frac{nN\pi e^4}{U_i^2}g^i \ , \tag{5}$$

where

$g^i = g(B;x)$.

In Fig. 7 we have plotted the satellite-to-parent intensity ratios on a normalized scale versus the reduced energy for P, Si, and Al. All data points were repeated a minimum of four times and the experimental data points for the three elements agree within ±2% at the higher energies. The solid curve is the normalized double- (g^{ii}) to single- (g^i) ionization cross-section ratios from Gryzinski's model, where $g^{ii} = g^{ii}_{sc} + g^{ii}_{ej}$. This latter curve was calculated for Si using $f = 1.35$ and $B = 3.3$. The value for B was obtained using Slater's rules as suggested by Robinson.[29] It gives a better estimate of the expectation value of the kinetic energy of the bound electron, although many investigators have used $E_1 = U_i$.[25] In the calculation of g_{ii}/g_i we have also included in g_i the single-ionization cross section contribution of the L_1 shell. For the L_1-shell value $B = 2.2$ was used. The rapid Coster-Kronig $L_1 L_{2,3} V$ transition should result in almost all the L_1 vacancies contributing to the total number of $L_{2,3}$ vacancies. This contribution lowers the value of the ratio g_{ii}/g_i by roughly 20%. We have neglected any other mechanism which might contribute to double ionization such as electron shake off. The general fit is good although the data peaks at $E_p/E_t \simeq 5$, while the peak in the theoretical curve occurs at 4.4. Some discrepancy at lower incident beam energies might be expected in comparing the functional dependence on E_p of the satellite-to-parent intensity ratios directly to g_{ii}/g_i, although it is believed to be small as discussed below.

For a normally incident electron beam of energy E_p, the Auger yield from a substrate for a particular transition can be written as[19]

$$I_{\text{Auger}} = G\,\text{Tr} I_0 (1-\omega) \int_0^\infty i(z)\, e^{-z/\lambda \cos\theta} dz \quad , \tag{6}$$

where G is the geometrical collection factor, T is the analyzer transmission, r is the secondary-electron enhancement factor, I_0 is the incident current, ω is the flourescent yield, λ is the mean escape depth for the Auger electrons, θ is the angle between the surface normal and the detector axis, and $i(z)$ is the ion density for the electron shell of interest ($L_{2,3}$ shell) as a function of depth per unit incident current. Since in the voltage range of the observed peak positions (800–1300 V), the range of the incident beam is much larger than the mean Auger-electron escape depth (the maximum Auger energy studied was 136 eV), we will assume that $i(z)$ is constant over the depth of region sampled by Auger spectroscopy. With this approximation we arrive at an expression which should reflect the true peak position very well. Hence, we take $i = nQ(E_p)$, where n is the atom density [we have taken $n(z) = n$] and $Q(E_p)$ is the ionization cross section as a function of energy. Thus we obtain the expression

$$I_{\text{Auger}} = G\,\text{Tr} I_0 (1-\omega) n Q \lambda \cos\theta \quad , \tag{7}$$

which has been used by other investigators for monolayer coverages.[22,30,31]

Now we make the assumption that the angular distributions for the Auger electrons in the parent and satellite peaks are identical and that these distributions are independent of the primary-electron energy. Then for the ratio of the Auger-satellite to the Auger-parent intensities we can write

$$\frac{I_s}{I_p} = \frac{r_s \lambda_s T_s Q_{II}}{r_p \lambda_p T_p Q_I} \quad , \tag{8}$$

where we have taken $(1-\omega_s)/(1-\omega_p) = 1$.[21]

We can simplify things by comparing the functional form of the above expression with the nor-

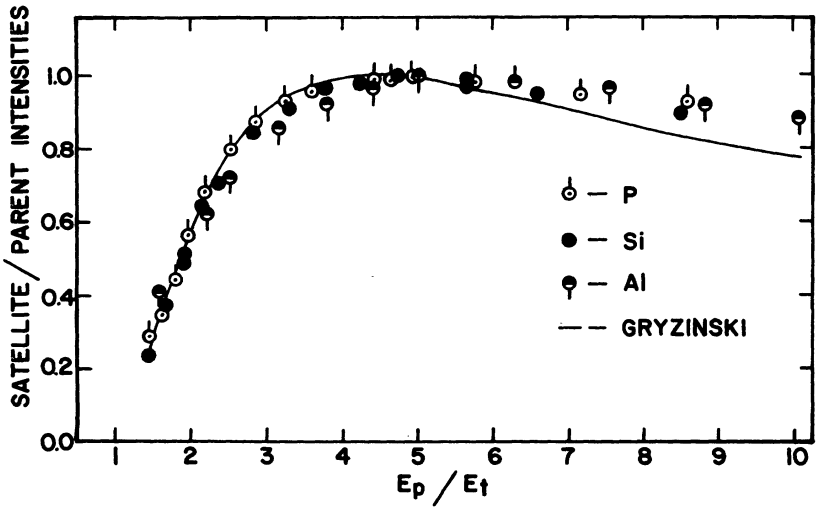

FIG. 7. Comparison of the normalized I_s/I_p ratio for Al, Si, and P with g_{ii}/g_i obtained by including single ionization of the L_1 shell plotted vs the reduced energy scale.

malized experimental data. Then we have simply $I_s/I_p \propto g^{ii}/g^i$ since $\lambda_s T_s/\lambda_p T_p$ is independent of E_p and r_s/r_p probably has a negligible E_p dependence. To see this, r can be written as $1+s$, where s gives the secondary-electron contribution to the total yield. For the voltage range used, s for Si has been found to vary slowly from 0.15 to 0.25 for the $L_{2,3}$ core level.[30,31] Hence any relative changes between s_s and s_p in the term $(1+s_s)/(1+s_p)$ will be small and will result in even a smaller change in the ratio.

Presented in Table III is a comparison of the absolute magnitudes of I_s/I_p and Q_{II}/Q_I made in the vicinity of the peak position ($E_p/E_t = 5.0$) for all three cases. The ratio of I_s/I_p is taken as the ratio of the product of peak-to-peak height and peak width squared as observed in the first derivative. In all cases ($V_{mod.}$ peak to peak)/(peak width at half-maximum) is on the order of 0.4. The ratios have been corrected for differences in the analyzer window width at the parent- and satellite-peak energies. Only the correction $r_p \lambda_p / r_s \lambda_s$ has not been applied. However, it should be close to unity. The corrected ratios are found to be in good agreement with those of Hanson and Arakawa.[7]

The ratio Q_{II}/Q_I has the form

$$\frac{Q_{II}}{Q_I} = \frac{(N-1)\pi e^4}{4\pi \tilde{d}^2 U_{ii}^2} \frac{g_{ii}}{g_i} , \tag{9}$$

where $\tilde{d}$ was calculated using the shell radius of L electrons given by Slater[32] and U_{ii} was taken to be given by $E_{L_{2,3}}(Z+1)$. The calculations based on Gryzinski's model are larger than the experimental data by a factor of about 2. The theory predicts a decrease in Q_{II}/Q_I with increasing Z, which is observed experimentally.

There appears to be some discrepancy between the magnitude of I_s/I_p for P and the other two samples. Instead of normalizing I_s/I_p as was done in Fig. 7, it should be possible to reduce the ordinate axis in the same manner as was done for the energy scale.[33] From Eq. (9) it is seen that this scale is proportional to the quantity $(I_s/I_p) r^2 U_{ii}^2$, where r is the L-shell radius. Calculating this quantity at the peak position ($E_p/E_t = 5.0$) we get 16.8 and 16.5 for Al and Si, respectively. However, for P a value of 13.4 is obtained. The disagreement is perhaps due to the fact that the principle Auger peak for P is quite broad and the parent and satellite structures do not seem to be clearly separated as can be seen in Fig. 4. In Fig. 1 and 2 the Al and Si satellites are clearly separated from the parent peaks.

TABLE III. Comparison of experimental data to the ratio of double to single $L_{2,3}$-shell ionization cross sections.

Material	I_s/I_p	$(Q_{II}/Q_I)\times\frac{1}{2}$
Al	0.0351	0.0318
Si	0.0234	0.0216
P	0.0145	0.0165

D. Ionization loss spectra of Si

A model for the plasmon-gain process has been discussed recently by Watts[11] and by Matthew and Watts[10] for the case of Auger transitions. This model was also discussed earlier by Hedin and Lundquist[34] for the case of x-ray emission and adsorption. In this model the satellites arise from Auger electrons emitted from atoms with excess energy in the form of valence-electron–core-hole coupling. This excess energy is of the order of the plasmon energy.

The result is pictured as an excited core state. A transition between an excited core state and a final state with no plasmon excitation is thought to yield the $L_{2,3}$ Auger-satellite band. Based on this model one expects a satellite-loss peak to be associated with the $L_{2,3}$ ionization-loss peak representing the excess energy ($E_{L_{2,3}} + \hbar\omega_p$) left with the excited atom. Also a correlation should exist between this higher-energy loss structure and the high-energy Auger satellite observed.

Indeed such a structure can be seen for Si at a loss energy 18-eV greater than the $L_{2,3}$ ionization-loss peak energy as previously reported by us[6] and as can be seen in Fig. 8. However, no apparent correlation exists between it and the satellite peak. In Fig. 5, at a beam energy of 250 eV, the $L_{2,3}$ loss structure is clearly visible in the $dN(E)/dE$ spectrum, although the Auger satellite at 107 eV is no longer evident. Hence it appears that this structure associated with the Si $L_{2,3}$ ionization-loss peak is a plasmon-loss satellite formed by primary electrons losing energy in inelastic collisions by exciting volume plasmons either before or after ionizing the $L_{2,3}$ core level. Indeed we have previously found that the ratio of the peak-to-peak heights of the silicon $L_{2,3}$ ionization loss peak and its associated plasmonlike-loss structure is in good agreement with the ratio of the first- to the second-bulk-plasmon loss of the primary peak. The ratios appear to be consistent with each other and this suggests that the same mechanism is involved.

A similar structure has been observed on the Si L_1 ionization-loss peak as can be seen in Fig. 8. Also, such loss structures were seen with P and Al but were not studied further.

If indeed the satellites arise from double ionization of the $L_{2,3}$ shell, one would expect to find a weak ionization-loss peak at the corresponding loss energy. Shown in Fig. 8 for Si is a dN/dE scan of the characteristic-loss spectrum with the elastic peak set at 600 V. Upon close examination

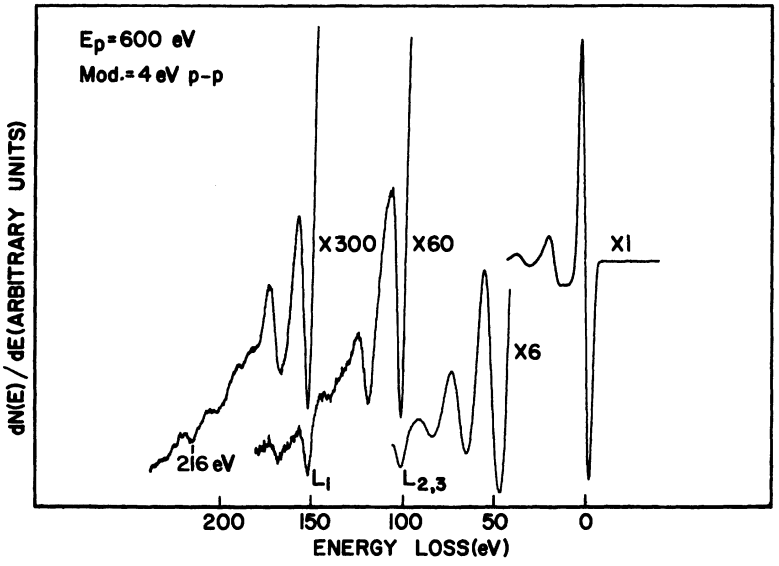

FIG. 8. Ionization-loss spectra for Si showing a structure at 216 eV tentatively identified as that corresponding to double ionization of the $L_{2,3}$ shell.

at a time constant of 10 sec (6 dB/octave), a loss structure was found at an energy 216-eV below the elastic peak. This corresponds well to that expected for double ionization. Also, the peak amplitude is of the correct order of magnitude. Its identity as a true loss peak can be verified simply by changing the beam voltage. It cannot be considered as a plasmon loss of the elastic peak since such peaks are clearly negligible in this energy range. Its only other possible identity is as an ionization-loss peak due to some impurity. However, other than a slight amount of carbon no other impurities were detectable.

Other peaks that can be easily identified in this spectrum are the L_1 ionization-loss peak and its associated plasmon loss. The $L_{2,3}$ ionization-loss peak can also be seen at a loss energy of 100 eV although the plasmon losses are relatively large at this energy.

A similar examination for such a peak for phosphorus and aluminum has not yet been made.

IV. CONCLUSIONS

In the present work Al, Si, SiO, and P were investigated with reagrd to their high-energy $L_{2,3}$ Auger-emission band satellites. The parent-satellite energy separation between like structures was determined using both $dN(E)/dE$ and $d^2N(E)/dE^2$ operating modes. Somewhat different results were obtained with the two methods. The results generally agree with the satellite shifts observed in x-ray emission spectra for Al and Si. The volume-plasmon energies measured for these samples agree well with other measurements and are consistently higher than the observed parent-satellite energy separation. No evidence was found that the energy separation ΔE for Si is dependent on the volume-plasmon energy of the sample.

The satellite threshold excitation energies were determined. An energy of $E_{L_{2,3}} + \hbar\omega_p$ expected from a plasmon-gain process was not observed. Rather the experimental energy cutoffs are much higher and correspond well to results expected for a double ionization of the $L_{2,3}$ shell.

It was found that the second derivative helped to reduce background but it did not entirely eliminate the need for making such corrections at the lower valotages where higher sensitivity had to be used. The uncertainty in these corrections also contributed significantly to the estimated uncertainty in the threshold energies.

The magnitude, E_p and Z dependence observed for the satellite-to-parent Auger intensity ratio was found to be in good agreement with the ratio of the double to single ionization cross section as given by Gryzinski's binary-encounter model.

The method of using ratios effectively helped to normalize generally unknown factors such as the secondary-electron enhancement factor and the mean escape depth. Also, it eliminated the problem involved in current normalization.

The previously reported plasmonlike-loss structure associated with the $L_{2,3}$ ionization-loss peak of Si was found not to be related to the high-energy Si $L_{2,3}$ Auger satellite. In addition, an ionization-loss peak for Si corresponding to double ionization of the $L_{2,3}$ shell is tentatively identified.

†Work supported by Air Force Contract No. AFOSR F-44620-69-C-0122.

*Present address: University of Wisconsin, Milwaukee, Wisc. 53201.

‡Present address: Physical Electronics Industries, Edina, Minn. 55435.

[1]L. H. Jenkins and M. F. Chung, Surf. Sci. 33, 159 (1972).
[2]M. F. Chung and L. H. Jenkins, Surf. Sci. 28, 409 (1971).
[3]B. D. Powell and D. P. Woodruff, Surf. Sci. 33, 437 (1972).
[4]H. G. MaGuire and P. D. Augustus, J. Phys. C 4, 1174 (1971).
[5]M. F. Chung and L. H. Jenkins, Surf. Sci. 26, 649 (1971).
[6]J. J. Melles, L. E. Davis, and L. L. Levenson, J. Vac. Sci. Technol. 10, 140 (1973).
[7]H. F. Hanson and E. T. Arakawa, Z. Phys. 251, 271 (1972).
[8]J. T. Grant and T. W. Haas, Surf. Sci. 23, 347 (1970).
[9]H. W. B. Skinner, Philos. Trans. Roy. Soc. London A 239, 95 (1940).
[10]J. A. D. Matthew and C. M. K. Watts, Phys. Lett. A 37, 239 (1971).
[11]C. M. K. Watts, J. Phys. F 2, 574 (1972).
[12]J. E. Rowe and S. B. Christman, J. Vac. Sci. Technol. 10, 276 (1973).
[13]M. Gryzinski, Phys. Rev. 138, A336 (1965).
[14]L. E. Davis, C. E. Bryson, III, J. J. Melles, J. E. Henson, and L. L. Levenson, J. Vac. Sci. Technol. 10, 564 (1973).
[15]P. W. Palmberg, G. K. Bohn, and J. C. Tracy, Appl. Phys. Lett. 15, 254 (1969).
[16]P. W. Palmberg, G. E. Riach, R. E. Weber, and N. C. MacDonald, *Handbook of Auger Electron Spectroscopy* (Physical Electronics Ind., Inc., Edina, Minnesota).
[17]L. E. Davis, L. L. Levenson, and J. J. Melles, J. Crys. Growth 17, 354 (1972).
[18]K. Ueda and R. Shimizu, Surf. Sci. 36, 789 (1973).
[19]P. W. Palmberg, Anal. Chem. 45, 549A (1973).
[20]J. J. Uebbing and N. J. Taylor, J. Appl. Phys. 41, 804 (1970).
[21]A. R. DuCharne and R. L. Gerlach, J. Vac. Sci. Technol. 10, 188 (1973).
[22]E. N. Sickafus and F. Steinrisser, J. Vac. Sci. Technol. 10, 43 (1973).
[23]E. H. S. Burhop and W. N. Asaad, *Advances in Atomic and Molecular Physics*, edited by D. R. Bates and I. Estermann (Academic, New York, 1972), Vol. 8, p. 164.
[24]J. R. Bearden and A. F. Burr, Rev. Mod. Phys. 39, 125 (1967).
[25]A. Burgess and I. C. Percival, in Ref. 23, Vol. 4, p. 109.
[26]G. Glupe and W. Mehlhorn, Phys. Lett. A 25, 274 (1967).
[27]D. N. Tripathi and D. K. Rai, J. Chem. Phys. 55, 1268 (1971).
[28]B. N. Roy, D. N. Tripathi, and D. K. Rai, Can. J. Phys. 50, 2961 (1972).
[29]B. B. Robinson, Phys. Rev. 140, A764 (1965).
[30]T. E. Gallon, J. Phys. D 5, 822 (1972).
[31]F. Meyer and J. J. Vrakking, Surf. Sci. 33, 271 (1972).
[32]J. C. Slater, *Quantum Theory of Matter* (McGraw-Hill, New York, 1968), p. 150.
[33]L. Vriens, *Case Studies in Atomic Collision Physics I*, edited by E. W. McDaniel, and M. R. C. McDowell, (North-Holland, Amsterdam, 1969), p. 337.
[34]L. Hedin and S. Lundqvist, *Solid State Physics*, edited by F. Seitz, D. Turnbull, and H. Ehrenreich (Academic, New York, 1969), Vol. 23, p. 2.